PAPER

# Novel design of honeybee-inspired needles for percutaneous procedure

Bioinspiration & Biomimetics

PAPER

# Novel design of honeybee-inspired needles for percutaneous procedure

RECEIVED
6 June 2017

REVISED
13 November 2017

ACCEPTED FOR PUBLICATION
20 December 2017

PUBLISHED
18 April 2018

Mohammad Sahlabadi and Parsaoran Hutapea
Department of Mechanical Engineering, Temple University, Philadelphia, PA 19027, United States of America
E-mail: hutapea@temple.edu

**Keywords:** bioinspired needle, honeybee stingers, insertion force, friction force, tissue damage, surgery needles, percutaneous procedure

## Abstract

The focus of this paper is to present new designs of innovative bioinspired needles to be used during percutaneous procedures. Insect stingers have been known to easily penetrate soft tissues. Bioinspired needles mimicking the barbs in a honeybee stinger were developed for a smaller insertion force, which can provide a less invasive procedure. Decreasing the insertion force will decrease the tissue deformation, which is essential for more accurate targeting. In this study, some design parameters, in particular, barb shape and geometry (i.e. front angle, back angle, and height) were defined, and their effects on the insertion force were investigated. Three-dimensional printing technology was used to manufacture bioinspired needles. A specially-designed insertion test setup using tissue mimicking polyvinyl chloride (PVC) gels was developed to measure the insertion and extraction forces. The barb design parameters were then experimentally modified through detailed experimental procedures to further reduce the insertion force. Different scales of the barbed needles were designed and used to explore the size-scale effect on the insertion force. To further investigate the efficacy of the proposed needle design in real surgeries, preliminary *ex vivo* insertion tests into bovine liver tissue were performed. Our results show that the insertion force of the needles in different scales decreased by 21–35% in PVC gel insertion tests, and by 46% in bovine liver tissue insertion tests.

## Introduction

In recent years, there have been a lot of research activities focused on designing innovative surgery needles for percutaneous procedures [1]. In particular, research on microscale bioinspired needles has garnered a lot of interest due to their potential applications in small biomedical devices [2,3]. However, to the authors' knowledge, there is limited research on mesoscale bioinspired needles (ranging from 0.1 mm to 5 mm), especially for needles used in minimally invasive surgeries [4]. Studies on bioinspired needles focusing on needle tip design and needle path controlling in medical robotics are also available in the literature, for example, in the work by Burrows *et al* [5]. In order to develop mesoscale surgical needles, especially for percutaneous procedures such as brachytherapy and cancer biopsy, understanding the mechanics of needle insertion, and exploring new needle shapes and geometries, are vital.

### Mechanics of needle insertion

Some important factors in needle insertion that are being explored by researchers are the geometry of the needle body and needle tip, material properties of the tissue, the speed of insertion, and the dynamics of the insertion, i.e. insertion with rotation and/or vibration. The survey done by van Gerwen *et al* [6] mentioned that there are more than 99 papers about tissue characterization; 38 of those utilized artificial tissue mimicking materials (i.e. polyvinyl chloride (PVC) and silicone gel phantoms), 8 papers used human tissue, and the rest studied animal tissues [7–10]. The speed of the insertion and its effects on insertion force and displacement of the tissue have been discussed by some researchers. For instance, some researchers investigated insertion velocity during clinical procedures [11, 12], while some inspected velocity effects in insertion in both artificial tissue mimicking materials [13–17] and biological tissues [18–20]. Other researchers have studied the dynamics

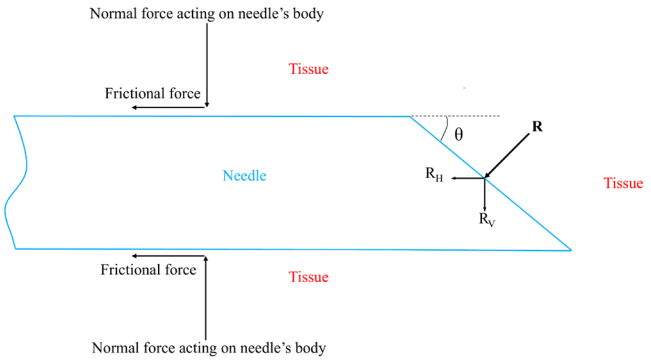


**Figure 1.** Force distribution on a bevel-tip needle during the insertion.

of insertion including the effects of needle rotation and vibration on the insertion force [21–24].

In addition, the influence of needle geometries and characteristics of needle–tissue interaction has been well investigated in recent years. For instance, the effect of the needle diameter on the insertion force was examined by Okamura *et al* [25], Shergold and Fleck [26], and Stellman [27]. They found that the geometry of the needle tip is an important factor during insertion that affects both the insertion force and the peak force. Bevel tip needles usually have less insertion force in comparison with needles with conical tips [6], and this fact affects new needle tip designs such that most of the designs are close to the bevel design. Mahvash and Dupont [1, 28, 29] have investigated the influence of needle lubricants on insertion force. They showed that lubricants significantly reduce the insertion force of steel surgical needles due to the reduction in the frictional force of the needle. Although there are several studies on needle diameter and tip geometries, few have tried to change the geometry of the needle body, which has always been a hollow cylinder [4].

There is always a desire among the medical community to improve the needle insertion performance. It has been determined that the shape and geometry of the needle has a big influence on the insertion force [25–29]. To deliver therapy or acquire biopsy samples for diagnostic purposes, the targeting accuracy of the needle is important. The insertion force, tissue deformation, and material properties of the tissue are main factors that affect needle targeting accuracy [6]. Among these factors, the insertion forces of conventional needles are relatively high, which causes placement inaccuracies [28]. The reduction in insertion force should be accompanied by a reduction in tissue deformation to potentially increase the targeting accuracy [30]. However, in this paper, our focus is to reduce the insertion force.

In our design, the needle body is modified to decrease the insertion force of the needle. Decreasing the insertion force decreases the damage to tissue [30]. There are also studies that suggest that reducing needle insertion force reduces pain [31, 32]. In minimally invasive surgeries, such as laparoscopic surgeries, operations are performed through small incisions instead of a big opening [33]. Although needle-based procedures are considered minimally invasive, damages caused by needle insertion into soft tissues, namely brain tissue, can cause long-lasting traumas and/or injuries [34]. Before getting into the details of the proposed honeybee-inspired needle design, more information on needle insertion force and honeybee stinger insertion mechanics is provided below.

### The ultimate insertion force and its components

The ultimate insertion force is defined as the force acting on the needle hub in the direction of insertion. The ultimate insertion force consists of the cutting force, friction force, and puncture force of the needle [6]. It has been discovered that the friction force is the largest contributor to the insertion force [35]. In our design, the focus is to decrease the insertion force of the needle by decreasing the friction force.

During a needle insertion, there are two kinds of reactive force acting on the needle–tissue interface. These forces are reactive normal and frictional forces. The reactive normal forces are perpendicular to the surface of the needle body. Conventional cylindrical needles have symmetrical geometries, which lead to a balance of normal forces acting on the needle's body. When pushed from the proximal end, a bevel-tip needle can gradually bend and follow a curved trajectory because of the lateral component ($R_V$) of the resultant force ($R$) experienced on the slant edge/area of the tip (figure 1). For needles with conical tips, the forces acting on the needle tip cancel each other out, which causes the needle to follow a straight path as it goes into the tissue. The focus of this paper is to study the geometry of the needle body, not the needle tip design. However, since needles with beveled or conical tips are most common, the insertion tests were performed with both tip designs to cover a wider range of applications.

### Honeybee stinger insertion mechanics

Insect stingers such as those shown in figure 2 have exceptional shape and geometrical features that facilitate insertion, and can be mimicked to design novel surgery needles. Some researchers have

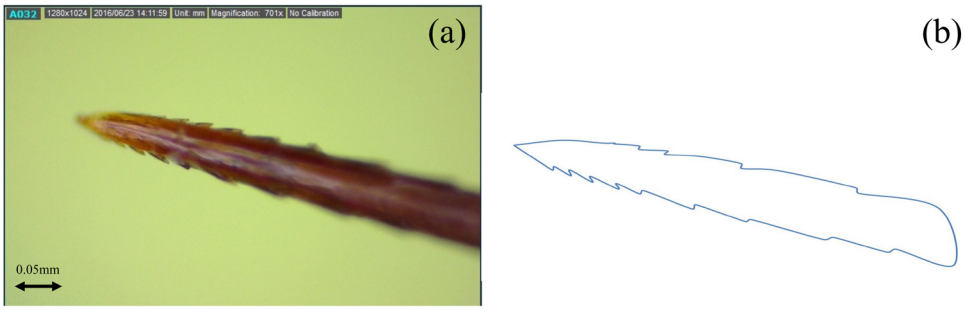


**Figure 2.** (a) The honeybee stinger, and (b) 2D drawing of the stinger obtained using ImageJ.

investigated honeybee stingers. For example, Ling *et al* [36] and Wu *et al* [37] separately studied the mechanics of the honeybee stinger and its barbs. Ling *et al* [36] concluded that the geometry of the stinger provides a relatively painless penetration into the human skin. Ling *et al* [36] reported that the average insertion force of the honeybee stinger is 5.75 mN, which it is about one order of magnitude smaller than that of an acupuncture microneedle. The insertion force of the stinger was significantly minimized due to a reduction in its friction force because of its barbs. The rupture force of the stinger was also decreased due to its ultrasharp tip. On the other hand, the average extraction force was about four times larger than the acupuncture microneedle extraction force. The extraction force was increased due to the mechanical interlocking of the barbs in the tissue. Wu [37] discussed the insertion mechanics of the honeybee stinger, and concluded that barbs in the stinger reduce the insertion force and also cause the stinger to rotate as it enters human skin.

Barbs in honeybee stingers have some advantages and disadvantages. Barbs cause the stinger to slightly rotate as it is inserted into tissue; this rotation facilitates a straight insertion and increases tissue damage. Barbs also decrease the insertion force of the stinger, which is favorable for us. Furthermore, the stinger's barbs increase the extraction force [31], increase the cutting force during insertion, are asymmetric, and their size increases from the tip to the bottom of the stinger. Needles with increasing cross-sectional areas and asymmetric geometries are hard to manufacture and steer; the reasons for this are discussed in the Materials and Methods section.

Inspired by the unique mechanics of the honeybee stinger, some preliminary studies on honeybee stingers were performed in our laboratory. A digital microscope (Dino-Lite, AnMo Electronics Corporation, New Taipei City, Taiwan) was used to take images of the honeybee stingers to help us learn more about their barb geometries. The images were then used to generate two-dimensional (2D) sketches of barb geometries and shapes (figure 2(b)).

In a honeybee stinger, barbs are located on two sides of the stinger with a 180° angular distance between them. They come out of the stinger main body as illustrated in figure 2. Since barbs come out of the stinger's body, they increase the cross-sectional area and the cutting force of the stinger as it advances into the skin and tissue. The density of the tissue, the speed of the insertion, and the cross-sectional area of the stinger perpendicular to the insertion direction are the parameters that affect the cutting force. Among these factors, the cross-sectional area depends on the needle's geometries. Barbs increase the cutting force and decrease the insertion force of the stinger; however, the increase in the cutting force is much smaller than the reduction in the insertion force because of the barbs. This explains why the total insertion force of the stinger decreases with barbs [36]. Moreover, as shown in figure 2(a), the back angle of the barbs in the honeybee stinger is too sharp, causing a higher extraction force [36].

Studying the insertion mechanics of the honeybee stinger and the effect of barbs on reducing the insertion force of the stinger inspired us to create a new honeybee-inspired needle design. In our honeybee-inspired needle, barbs are added to the needle design to reduce the ultimate insertion force. The design of the honeybee-inspired needle and its barbs will be discussed in detail in the Materials and Methods section. To see the effectiveness of the proposed barbed needle design to decrease the insertion force, insertion tests into tissue mimicking PVC gels were performed (the reasons for utilizing PVC gel, and its properties, will be discussed in the Experimental Procedure section). The effects of the barbs' design parameters on needle insertion and extraction forces were investigated, and the parameter values were experimentally modified to further reduce both insertion and extraction forces. The size-scale effect on the insertion force was explored. Finally, insertion tests into bovine liver tissue were carried out to show the efficacy of the proposed design.

The outline of this paper is as follows. The Materials and Method section discusses the honeybee-inspired needle design, three-dimensional (3D) modeling and manufacturing of the honeybee-inspired needles, and the experimental procedure. The Results section provides insertion and extraction forces results for the barbs' design parameters modification study, barbed needles scale study, and insertion tests into bovine liver tissue. The Discussion section gives a summary of the

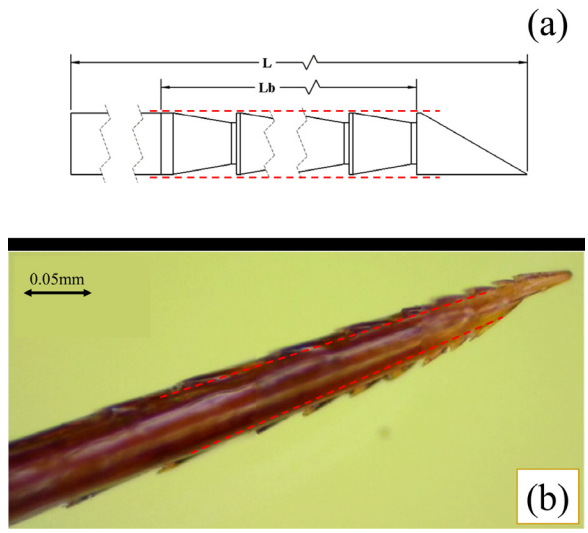


**Figure 3.** (a) Design of the barbs in a barbed needle (barbs are inside the outer diameter of the needle body) ($L$ = length of the needle, $L_b$ = length of the barbed section), and (b) barbs in a honeybee stinger (barbs are added to the main body of the stinger).

study, including a discussion on the manufacturability of the proposed needle design. Finally, the Conclusion section demonstrates the effectiveness and importance of the new needle design, offers creative approaches to the problem, and suggests some of the potential medical applications of the proposed design.

## Materials and methods

### Honeybee-inspired needle design

Considering all pros and cons of the barb geometry in a honeybee stinger, novel needle designs with barbs inspired by the barbs in honeybee stingers are proposed. Our concept is illustrated in figure 3(a). The design presented in this work maintains the advantage of the stinger's barbs to reduce the insertion force while at the same time aims to reduce or eliminate any disadvantages, namely the high extraction force of the stinger. The new design of the barbs in our honeybee-inspired needles are not going to be exactly like the barbs in the stinger.

In our design, barbs are created in the body of the needle so that they do not increase the cross-sectional area of the needle and its cutting force in insertion. When it comes to adding barbs to a needle design, the extraction force of the needle is a great concern. However, the barb geometries in our design are carved on the needle's body, which reduces the contact area between the back of the barbs and the tissue during extraction (figure 3(a)). It is conjectured that the barbs will not cause an increase in the extraction force.; Extraction tests were performed to validate this hypothesis.

Honeybees sting to protect themselves and their hives against predators. Their stingers are asymmetric, which causes placement inaccuracy; however, this is not an issue for them since honeybees, unlike mosquitos, do not need to reach a specific target (e.g. a blood vessel) inside their prey's or predator's body [38].

Having symmetry is critical for mesoscale (ranging from 0.1 mm to 5 mm, which includes surgical needles such as hypodermic and biopsy needles) honeybee-inspired needles; this is because any asymmetric section in a needle will generate forces on the needle body, which causes the needle to bend and deviate from its target. In an axisymmetric needle, the forces acting on the needle body cancel each other out. Having less or no normal forces acting on the body helps us to control the needle path inside the tissue much easier. The manufacturability of a symmetric design is also higher than an asymmetric design due to the simplicity of barb geometries. Symmetric barb geometries can be carved out of surgical needle bodies using a mesoscale computer numerical control machine; this means that barb designs can be applied to different surgical needle/electrode designs with different medical applications. Moreover, as mentioned earlier, barbs in the honeybee stinger cause the stinger to slightly rotate during insertion, which increases tissue damage and is not beneficial for us [36]. Therefore, in our design, the barbs revolve 360° around the center line to generate a symmetrical geometry for the body (figures 3 and 4). The shape of the tip (which could be either beveled or conical) was added to the design at the end (figure 4).

The design parameters of the barbs are the front ($\theta_1$) and back ($\theta_2$) angles of the barb, barb height ($h$), barb tip thickness (which indicates the sharpness of the barb tip) ($t_1$), and the length of the section with barbs ($L_b$). The length of the section with barbs ($L_b$) is shown in figure 3(a), and the rest of the parameters are illustrated in figure 4.

3D models of the barbed and conventional needles with beveled and conical tips generated using CAD software are illustrated in figure 5(a). Fifty-five needles were manufactured using a Connex350 3D printer (Stratasys, Inc., Eden Prairie, MN), as shown in figure 5(b) and table 1. The Connex350 3D printer has a high-resolution print layer accuracy of 16 $\mu$m.

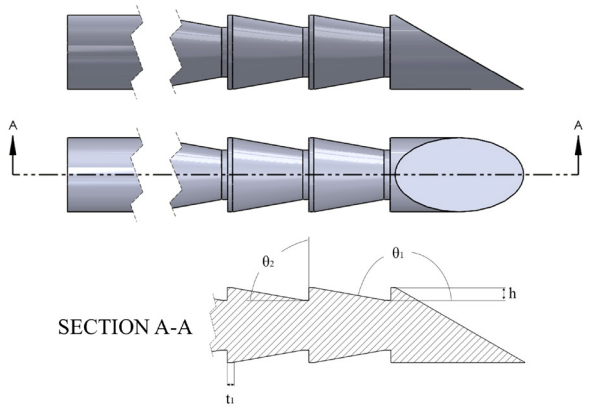


**Figure 4.** Barb design parameters.

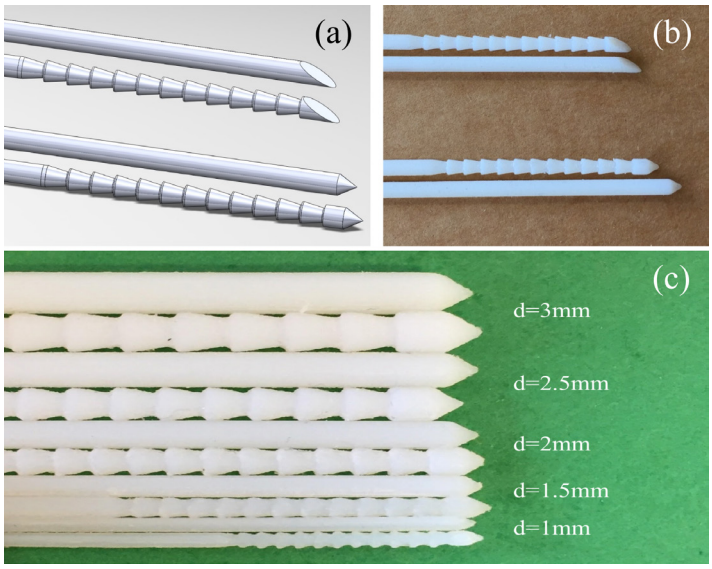


**Figure 5.** (a) 3D models of the conventional and barbed needles, (b) 3D printed needles with a diameter of 3 mm, and (c) 3D printed needles with different diameters.

**Table 1.** Classification of the needles used in this paper based on their types and tips.

| *Total* number of needles: 55 | | | |
|---|---|---|---|
| Conventional needles: 13 | | Barbed needles: 42 | |
| Bevel-tip needles:5 | Conical tip needles:8 | Bevel-tip needles: 18 | Conical tip needles:24 |

**Table 2.** Needles dimensions.

| $d$ (mm) | $L$ (mm) | $\theta_1$ | $\theta_2$ | $h$ (mm) | $L_b$ (mm) | $t_1$ (mm) |
|---|---|---|---|---|---|---|
| 3 | 180 | 90°, 100°,110°, 120°, 130°, 150°, 170° | 90°, 110°, 130°, 150°, 160°, 170° | 0.1, 0.2, 0.3, 0.4, 0.5 | 10, 20, 30, 40, 50,60 | 0.05,0.1,0.15,0.2, 0.25 |

The material used to make these needles is a polymer, which consists of 30% acrylic monomer, 25% isobornyl acrylate, 15% phenol, 12% diphenyl-2, 8% titanium dioxide, 5% acrylic acid ester, and 5% a composition of phosphoric acid and propylene glycol monomethyl ether acetate. Table 2 represents all design parameter values of the needles used in this work.

The scaled-up needles with a diameter of 3 mm were used to explore the barbed needles' insertion mechanics and to learn more about the barbs' design parameters' influences on insertion force. To investigate the size-scale effect on the insertion force, the needle with modified design parameter values was scaled down to five different scales, as shown in figure 5(c); these needles were used to for insertion tests into PVC gels.

Although the magnitude of the insertion force may change using needles with different material properties,

all needles (barbed and conventional needles) that were tested were manufactured using the same material. Therefore, the effect of needle geometries on final insertion forces remains independent of the material properties since the same material is consistently used. The conical needles will follow a straight path in insertion, and therefore the extraction force data obtained for them will be much cleaner and more accurate than for bevel-tip needles. The barb heights vary from 0.1 to 0.5 mm, and the ratio of barb height to needle diameter varies from 0.13 to 0.33. The ratio of the barb to stinger diameter for the honeybee stinger varies from 0.14 to 0.25.

Adding barbs to needle designs will decrease the bending stiffness of the needles. The bending stiffness of the conventional and barbed needles were estimated using results obtained from bending tests. To do so, both needles were designed and manufactured using a CAD software and a Connex350 3D printer (Stratasys, Inc., Eden Prairie, MN). A concentrated sheer force ($P$) of 0.02 N was applied to the ends of needles. The results obtained from bending tests are presented in the Results section.

Another issue in insertion is buckling of the needle, which can be controlled using a needle guider. The guider decreases the unsupported length of the needle (which is the most effective parameter in buckling strength), and increases the buckling strength. Having barbs decreases the buckling strength; the level of reduction depends on barb height. The buckling equation is $F_b = (\pi^2 * E * I)/(L_{eff})^2$, in which $F_b$ is the critical buckling force, $E$ is the modulus of elasticity, $I$ is the area moment of inertia, and $L_{eff}$ is the effective length. The effective length is $L_{eff} = K * L$, where $K$ is the column effective length factor, and $L$ is the unsupported length factor. For a barbed needle with barb height of 0.1 mm, the cross-sectional diameter varies from 2.8 to 3 mm. Therefore, the buckling strength of a conventional needle with a diameter of 2.8 mm is equal to the lowest buckling strength that a barbed needle with a diameter of 3 mm and barb height of 0.1 mm can have. To simplify the calculation process, the buckling strengths of conventional needles with diameters of 2.8 mm and 3 mm were compared. This is like considering the most severe possible outcome (worst-case scenario) that could happen for a barbed needle in terms of its buckling strength. Using the buckling equation, the critical buckling force for a conventional needle with a diameter of 2.8 mm was estimated to be 76% of that for a conventional needle with a diameter of 3 mm. Moreover, from our results we know that using a barb height of 0.1 mm in a needle with diameter of 3 mm reduces the insertion force by 17%; this means that the barb effect on decreasing the buckling strength of the needle (a 14% reduction) is smaller than the decrease in insertion force of the needle (a 17% reduction) because of the barbs.

Due to the reduction in surface area, the barb design of the needle naturally reduces the frictional surface between the needle and surrounding tissue, which results in a reduction in the friction force of the needle during insertion and extraction. The friction force of the needle has the largest contribution to the ultimate insertion force; therefore, decreasing the friction force considerably reduces the insertion force. This assumption will be investigated through this study.

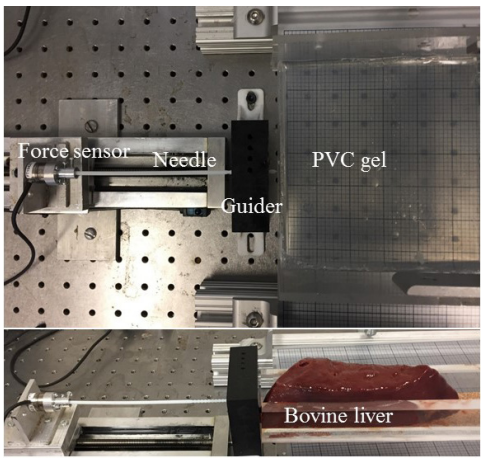


**Figure 6.** The insertion test setup.

## Experimental procedure

The insertion test setup included a linear motor to provide translational motion, a force sensor, a programmable data acquisition system to record the insertion force, and either a PVC gel or bovine liver tissue (see figure 6). The force sensor was a six-axis Force/Torque Transducer Nano17® (ATI Industrial Automation, Apex, NC). The force sensor was connected to a data acquisition system, and insertion force data were acquired using LabVIEW software (National Instruments Corporation, Austin, TX). The maximum insertion depth of the needles was 7 cm. The insertion velocity in our tests was 1.5 mm $s^{-1}$ to decrease tissue damage. The majority of the insertion speeds used in the literature were in the order of 1–10 mm $s^{-1}$ [6]. In general, having a higher insertion speed decreases the puncture force and initial tissue displacement, but increases the friction force [6, 18]. However, increasing the insertion speed in soft tissues decreases the friction force and increases tissue damage due to the fact that needles with a higher insertion speed make bigger holes inside the tissue [39]. Therefore, a lower insertion speed for insertion into soft tissues, such as brain tissues, should reduce the potential damage.

Insertion tests were done using PVC gel phantoms, which have been commonly utilized to mimic elastic properties in tissue [40]. The Young's modulus and density of PVC gels were 3.5KPa and 1.1 g $cm^{-3}$, respectively [41]. The PVC gel's mechanical behavior is close to that of elastic tissues, namely liver tissue [40]. Therefore, the results acquired from insertion tests into PVC gels are a good representation of the

needle–tissue interaction for insertion into liver tissue. Since our work is a comparative geometrical study, the possible error of using PVC gel instead of a biological tissue will not be significant; however, insertion tests into biological tissues should be done to show relevance for real applications. PVC and softener were combined to mimic the viscoelastic properties of tissue. The mixed solution was heated until the PVC plastic became activated, resulting in a thick solution that solidifies when cooled. This viscous liquid was poured into metal molds and placed in a freezer until fully solidified.

One conventional needle (with $d = 3$ mm and $L = 180$ mm), and three different barbed needles (with $d = 3$ mm, $L = 180$ mm, $h = 0.5$ mm, $t_1 = 0.2$ mm, $\theta_2 = 110°$, and different front angles of $\theta_1 = 110°$, 130°, and 150°) were manufactured using the Connex350 3D printer (Stratasys, Inc., Eden Prairie, MN) (figure 3(a)), and were then used for insertion tests into tissue-mimicking PVC gels. First, tests were performed using needles with our initial barb designs to prove the concept. Our preliminary results showed that the insertion force was decreased by 25% using barbed needles, regardless of the barb geometry and design parameter values [42–45]. These results motivated us to further study the barbs' design parameters' effects on the insertion and extraction forces.

To investigate the effect of each design parameter on insertion and extraction forces, the influence of each parameter on the insertion force was explored separately while the other design parameters were kept constant. Then, each parameter was modified based on maintaining the minimum insertion/extraction force. Insertion forces of needles with different values for one parameter (and fixed values for other parameters) were compared to one another, and the value that gave us the minimum insertion force was chosen to be the modified value for that parameter. For example, the first series of experiments were done using seven samples with different barb front angles ($\theta_1$) and fixed values for other design parameters ($\theta_2 = 90°$, $h = 0.5$ mm, and $L_b = 30$ mm). By testing needles with different front angles ($\theta_1$), the effect of this parameter on the insertion force of the needle was explored. The needle with $\theta_1 = 170°$ had the minimum insertion force among all needles tested in that set of experiments. The barb front angle was then modified to $\theta_1 = 170°$ in an effort to further reduce the final insertion force. The second set of experiments used 12 samples with different barb back angles ($\theta_2$) and fixed values for other design parameters ($\theta_1 = 170°$, $h = 0.5$ mm, and $L_b = 30$ mm). The back angle ($\theta_2$) was also modified following the same procedure as discussed above. The process was repeated for the third, fourth, and fifth sets of experiments. The barb back angle was the only parameter that was studied and modified for both insertion and extraction forces, mainly due to its effect on the extraction force [36].

The size-scale effect on insertion force results was explored using five scaled-down versions of the needle with modified barb design parameters values (figure 5(c)). The insertion tests were performed using PVC gels.

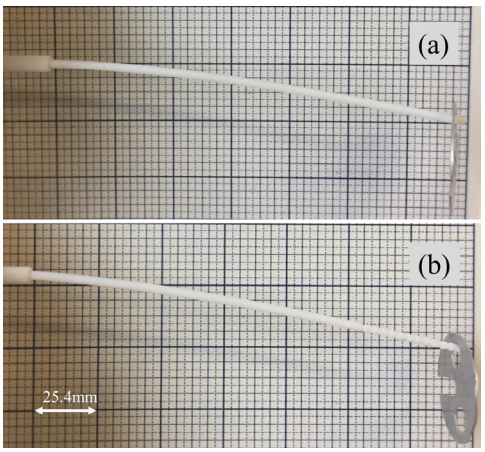


**Figure 7.** The bending tests using (a) conventional, and (b) barbed needles.

To show relevance for real applications, *ex vivo* insertion tests into bovine liver tissue were also performed using two different scales of the modified needle, $d = 2$ mm and $d = 3$ mm, respectively. A specially designed box was utilized to hold liver tissue during the insertion (figure 6).

## Results

The insertion tests into tissue-mimicking PVC gels and bovine liver tissue were carried out using barbed and conventional needles. The insertion and extraction forces results are presented in this section.

### Bending tests

The deflections ($w$) of conventional and barbed needles were measured to be 25.4 mm and 27.1 mm, respectively (figure 7). The bending stiffness ($K = P/w$) was calculated using deflections data; it was 0.78 N m$^{-1}$ for the conventional needles, and 0.74 N m$^{-1}$ for the barbed needles. These results showed a 5% decrease in the bending stiffness for the barbed needle. Since the insertion force decreased by at least 17% using barbed needles (based on our insertion test results presented in the Results section), the 5% reduction in bending stiffness is negligible.

### Effect of front angle on insertion force

The effect of the front angle ($\theta_1$) on the insertion force of the needle was studied in our first set of experiments. Figure 8 shows the averages of three trials for the insertion tests of needles with different barb front angles ($\theta_1$). The insertion forces for the conventional needle and the needles with front angles of 90° and 100° are almost identical. It is conjectured that the frictional surface, that is, the surface around the needle, is almost the same for both types of needles. In needles with a barb front angle of 90°, the barbs are

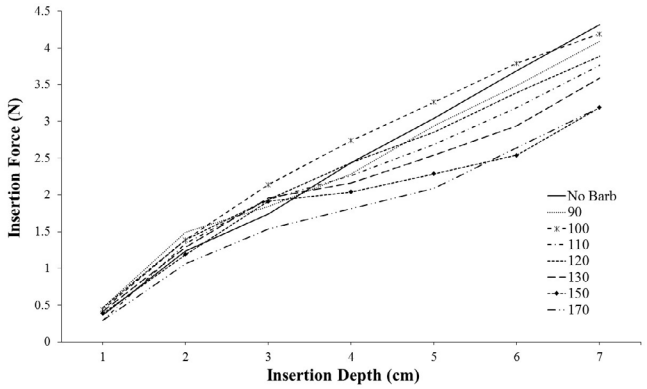


**Figure 8.** Insertion force versus insertion depth results for bevel-tip conventional needle and barbed needles with different barb front angles ($\theta_1$), and for $\theta_2 = 90°$, $h = 0.5$ mm, $L_b = 30$ mm, and $t_1 = 0.2$ mm.

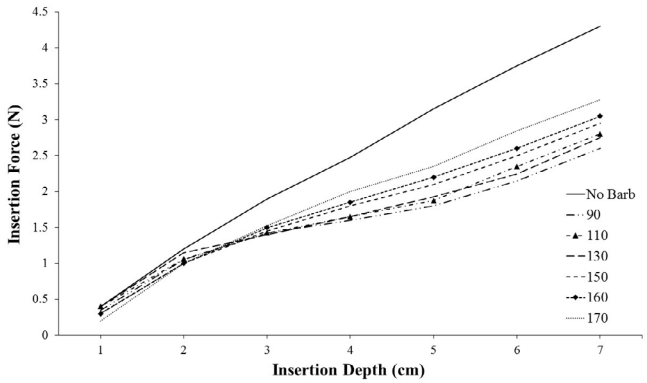


**Figure 9.** Insertion force versus insertion depth results for conical tip conventional needle and barbed needles with different barb back angles ($\theta_2$), and for $\theta_1 = 170°$, $h = 0.5$ mm, $L_b = 30$ mm, and $t_1 = 0.2$ mm.

very close to one another, and the gap space between two barbs is too small; therefore, the overall reduction in the frictional surface is not significant. As the front angle changes from 100° to 110°, the gaps between the barbs start to widen, which means the frictional surface decreases, leading to less insertion force. As the front angle increases from 110° to 170°, the frictional surface decreases, which results in further reduction in the insertion force. The insertion force reaches its minimum value for the needle with the front angle of 170°. However, this may not be the overall minimum since increasing the front angle decreases the frictional surface of the needle, and this reduction is independent of other parameter values. The trend observed in this set of experiments could be seen for any combination of other values ($\theta_1$, $h$, $L_b$, $t_1$). The insertion force was decreased by 27% on average, and by 28% at an insertion depth of 7 cm, using a barbed needle with a front angle of 170°. A small standard deviation value represents the consistency of the results. The average standard deviation values estimated for needles with different front angles did not exceed 0.19.

### Effect of back angle on insertion and extraction forces

We studied the effect of back angle ($\theta_2$) on the frictional force during needle insertion. For example, it is hypothesized that a very wide back angle increases the frictional surface and insertion force of the needle. The effect of back angle on the extraction force of the needle is also important, since the main concern about using barbs in needle design is the high extraction force.

The average insertion forces of three trials for conical tip needles with a barb front angle of 170°, and six different barb back angles ($\theta_2 = 90°$, 110°, 130°, 150°, 160°, and 170°) are shown in figure 9. The results are consistent since the average standard deviation values are less than 0.17. There is a considerable reduction in the insertion force when using the barbed needle compared with the conventional needle. As shown in figure 9, the insertion forces of the needles with different barb back angles are close to one another; in other words, the variation in insertion force with the barb back angle is relatively small. Although the effect of the back angle on the insertion force is not significant, the back angle of 90° has the minimum insertion force. Using the needle with a back angle of 90°, the insertion force was decreased by as much as 23% on average, and by 25% at the insertion depth of 7 cm for a cone-shaped needle tip. This is because it creates the greatest gap space, as displayed in figure 10(a). As the barbed needle with a back angle of 90° (figure 10(a)) advances into the gel, the surrounding gel moves from one barb

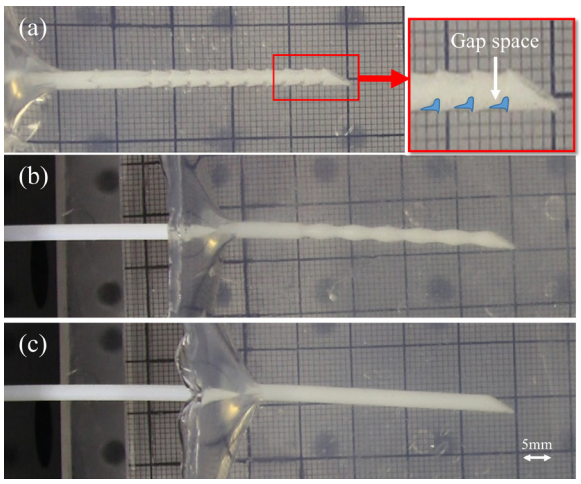


**Figure 10.** Effect of barb back angle on insertion force of the needle, for needles with back angles of (a) $\theta_2 = 90°$ and (b) $\theta_2 = 170°$, and (c) the conventional needle.

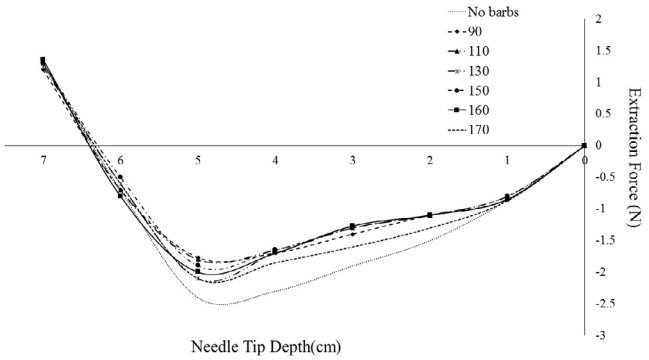


**Figure 11.** Extraction force versus needle tip depth results for the conical tip conventional needle and barbed needles with different barb back angles ($\theta_2$), and for $\theta_1 = 90°$, $h = 0.5$ mm, $L_b = 30$ mm, and $t_1 = 0.2$ mm.

to another without going into the gap space in between those two consecutive barbs; this causes a significant reduction in the contact surface (between the needle and gel) and the friction force. The gap space created during insertion of the needle with a back angle of 90° (figure 10(a)) is larger than those of the needle with a barb back angle of 170° and the conventional needle (figures 10(b) and (c)). The modified back angle should be 90° based on the insertion tests results. However, to find the modified back angle that decreases both insertion and extraction forces, results for the extraction force are also required.

The extraction starts right after the insertion (and at an insertion depth of 7 cm). The average standard deviation values for the extraction tests are less than 0.15. During insertion, the deformed gel pushes back the needle, which is why the insertion data shows a positive insertion force of 1.5 N (figure 11). As the needle is being extracted, both the needle and the gel move backward together, and thus the friction force read in this part is the static friction force. At an insertion depth of 5 cm, the coefficient of static friction reaches its maximum (which corresponds to the maximum friction and extraction force), and then the gel starts to slide over the needle body. During the last part of the experiments, the coefficient of kinetic friction is fixed while the length of the needle inside the gel is decreasing; this decreases the extraction force to zero as the needle is pulled out of the gel. As presented in figure 11, the extraction forces of the needles with barbs are less than those of conventional needles. In our design, barbs are created inside the outer diameter of the needle, and therefore the extraction force of the needle decreases due to the reduction in the frictional surface between the needle and the phantom gel. The extraction forces data obtained for barbed needles with different barb back angles are close to one another, which means the variation of the extraction force with the barbs' back angle is small. The maximum reduction in insertion force in this set of experiments is achieved by using the needle with the back angle of 90°. In summary, based on both insertion and extraction forces determined for the needles with different barb back angles, the modified back angle is 90°.

### Effect of barb height on insertion force

Since larger barb height decreases the frictional surface, studying the effect of barb height on the insertion force

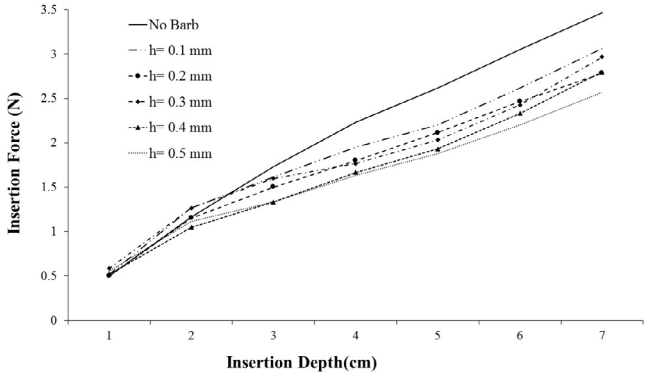


**Figure 12.** Insertion force versus insertion depth results for bevel-tip conventional needle and barbed needles with different barb heights ($h$) ($\theta_1 = 170°, \theta_2 = 90°, L_b = 30\,\text{mm}$, and $t_1 = 0.2\,\text{mm}$).

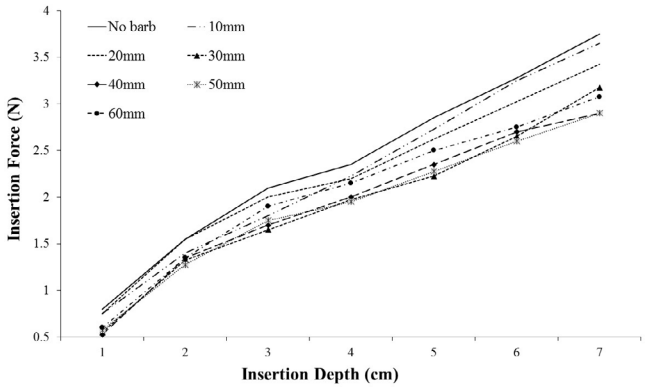


**Figure 13.** Insertion force versus insertion depth results for bevel-tip conventional needle and barbed needles with different lengths of barbed sections ($L_b$) ($\theta_1 = 170°, \theta_2 = 90°, h = 0.5\,\text{mm}$, and $t_1 = 0.2\,\text{mm}$).

of the needle is important. Increasing the barb height also decreases the bending stiffness of the needle; however, by knowing the effect of barb height on the insertion force of the needle, and choosing a proper value for the barb heights, a desirable needle insertion force and bending stiffness will be achieved. Figure 12 represents the average insertion force of three trials for conventional needles and needles with different barb heights while the barb front and back angles are 170° and 90°, respectively. The average standard deviation values for the needles with different barb heights do not go beyond 0.1. As shown in figure 12, the insertion force for the conventional needle is much higher than that of barbed needles. Furthermore, for the barbed needles, the insertion force for needles with the barb height of 0.5 mm is less than that of needles with smaller barb heights. This is because for the needle with a larger barb height, the contact between the needle's surface and PVC phantom gel decreases, which results in a smaller frictional surface and insertion force. Using the needle with the barb height of 0.5 mm, the insertion force is reduced by 25% on average, and by 28% at the insertion depth of 7 cm. It was observed that even for the barb height of 0.1 mm, the insertion force is decreased by 17% at the insertion depth of 7 cm. This demonstrates that adding even a very small barb would decrease the insertion force significantly; meanwhile, while the reduction in the needle's bending stiffness is negligible.

### Effect of the length of the barbed section on insertion force

The effect of the length of the barbed section ($L_b$) (figure 3(a)), is studied because it can be assumed that a larger $L_b$ should correspond to both less friction and insertion force. Here, a modified value for barb length ($L_b$) is determined by evaluating which needles would give a significant decrease in the insertion force. The effects of the barb length on the insertion force are investigated using the barbed needles with different $L_b$, and the average standard deviation values are less than 0.17. Based on the results obtained at the insertion depth of 7 cm, the maximum insertion force of the needle with $L_b = 10\,\text{mm}$ and the conventional needle are almost the same. For the needle with $L_b = 20\,\text{mm}$, the maximum insertion force starts to decrease. Needles with $L_b = 30\,\text{mm}$ and $L_b = 60\,\text{mm}$ reduce the maximum insertion force by 24% and 27%, respectively. Using needles with $L_b = 40\,\text{mm}$ and $L_b = 50\,\text{mm}$ result in a 35% reduction in the maximum insertion force. Since a longer $L_b$ corresponds to a lower bending stiffness of the needle, the modified value of $L_b$ is considered to be the smallest value of $L_b$ that gives the maximum reduction in the insertion force. In this

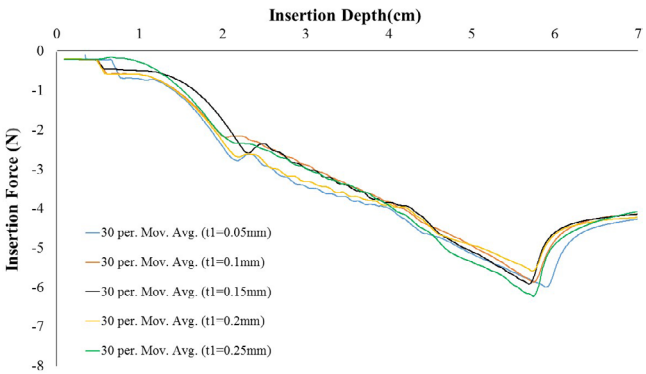


**Figure 14.** Insertion forces results for the insertion tests into PVC gels using barbed needles with different barb tip thicknesses ($t_1$) ($\theta_1 = 170°, \theta_2 = 90°, h = 0.5\,\text{mm}$, and $L_b = 40\,\text{mm}$).

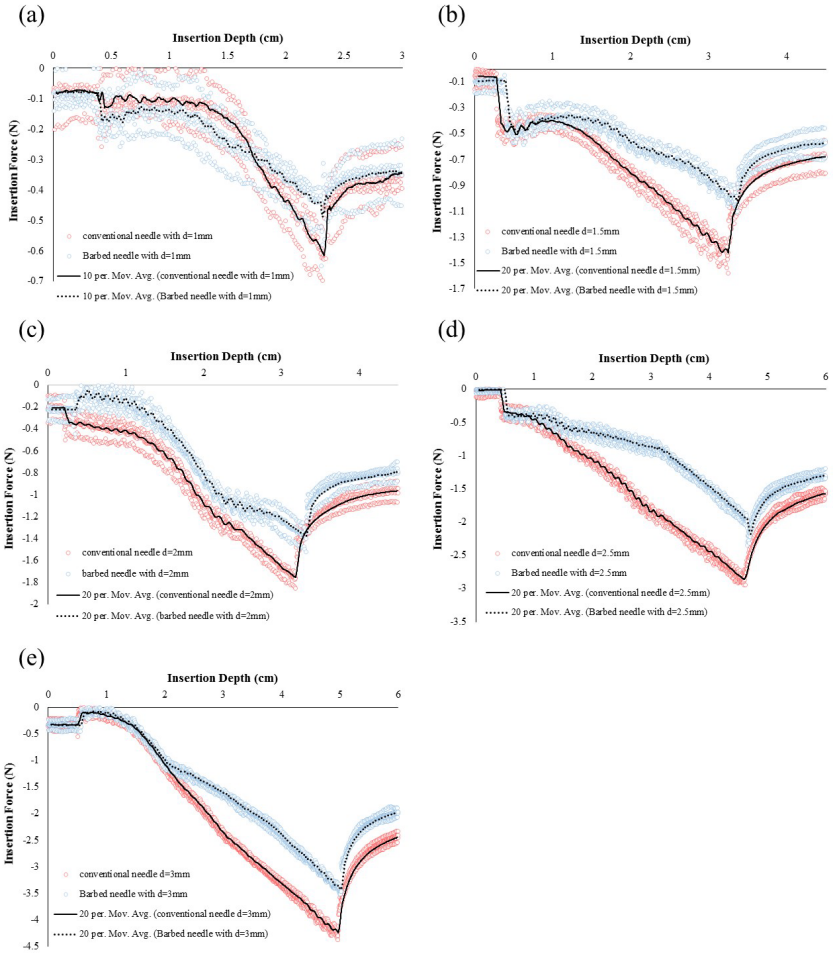


**Figure 15.** (a) The insertion forces obtained from the insertion tests into PVC gels for barbed and conventional needles with (a) $d = 1\,\text{mm}$, (b) $d = 1.5\,\text{mm}$, (c) $d = 2\,\text{mm}$, (d) $d = 2.5\,\text{mm}$, and (e) $d = 3\,\text{mm}$.

case, based on the results presented in figure 13, the modified barbed section length ($L_b$) is 40 mm.

### Effect of barb tip thickness on insertion force

The effect of barb tip thickness ($t_1$ in figure 4) on the insertion force of the needle was explored. Insertion tests into PVC gels were performed using needles with different barb tip thicknesses ($t_1 = 0.05, 0.1, 0.15, 0.2$, and $0.25\,\text{mm}$). As shown in figure 14, the insertion forces obtained for all needles are similar, which means the thickness of the barbs does not affect the insertion force of the needle. Needles with different barb tip thicknesses have the same frictional surfaces, and therefore they are all expected to have the same insertion force. In other words, the gap space between two consecutive barbs is a function of parameters like barb front and back angle, and barb height, and the sum of all gap spaces will affect the insertion force; by looking at the barb geometry shown in figure 4, it can be concluded that barb tip thickness affects neither the

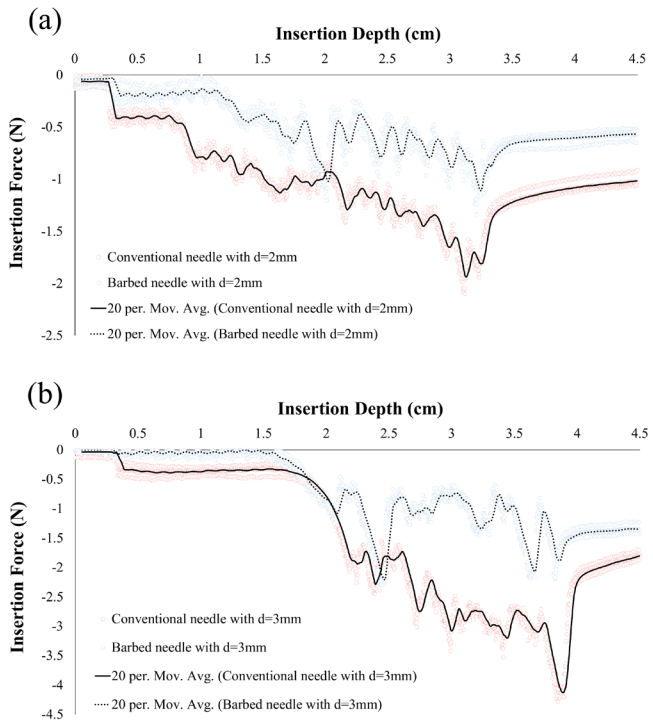


**Figure 16.** (a) the insertion forces acquired from the *ex vivo* insertion tests into bovine liver tissue using barbed and conventional needles with (a) $d = 2$ mm, (b) $d = 3$ mm.

gap space nor the insertion force. The average standard deviation values calculated for needles with different barb tip thicknesses do not exceed 0.19.

All design parameters' influences on the insertion force of the needle were investigated, and their values were modified to further reduce the needle insertion force. Using the needle with modified barb parameters reduced the insertion force by 35%, which is the lowest insertion force among all needles used in this study so far.

### Size-scale effect on insertion force

Since all the experiments were done using a scale-up model of the barbed needle, a scaling study was also performed to explore the effectiveness of the barbed design in smaller scales. Barbed needles with different outer diameters/scales were manufactured and tested using PVC gels, and their results were compared to those attained for conventional needles of the same sizes (figure 15). The barbed needles used in this set of experiments are scaled-down versions of the needle with modified barb parameters. As shown in figure 15, the insertion forces of the barbed needles in all scales are less than those of the conventional needles. The maximum insertion force reduction acquired using barbed needles in different scales are as much as 25% for needles with $d = 1$ mm, 26% for needles with $d = 1.5$ mm, 21% for needles with $d = 2$ mm, 24% for needles with $d = 2.5$ mm, and 23% for needles with $d = 3$ mm. Each insertion force curve presented in figure 15 is the average of the results obtained from three trials. The average standard deviation values determined for the insertion force data are 0.06 for $d = 1$ mm, 0.09 for $d = 1.5$, 0.1 for $d = 2$ mm, 0.11 for $d = 2.5$, and 0.14 for $d = 3$ mm.

### Insertion tests into bovine liver tissue

The PVC gels used throughout this study are homogenous, and are widely used to mimic biological tissue properties. However, to show the relevance for real applications, preliminary *ex vivo* insertion tests into bovine liver tissue were performed using barbed and conventional needles in two different scales with $d = 2$ mm and $d = 3$ mm, respectively. As shown in figure 16, the insertion forces of the needles in both scales decrease using barbed needles. The reduction in the maximum insertion forces of both barbed needles with $d = 2$ mm and $d = 3$ mm is as much as 46%, which is significantly higher than force reductions in PVC gel insertions. The average standard deviations estimated for the insertion forces data in insertion into bovine liver tissue are 0.15 for the needles with $d = 2$ mm, and 0.19 for the needles with $d = 3$ mm.

The bioinspired needle designs used in our research, and all the barb design parameter values are presented in table 3. The bold values in table 3 are the modified values obtained from different sets of experiments. The range of the average standard deviations calculated for different sets of experiments are also presented in table 3.

## Discussions

It has been demonstrated that the proposed honeybee-inspired needles decrease both insertion and extraction forces due to the reduction in frictional surface of the needle. In this study, design parameters of the barbs were

**Table 3.** Bioinspired needle design parameters. Underlined values are modified values based on minimum insertion and extraction forces.

| Effects of barbs' design parameters on insertion/ extraction forces | Number of the conventional needles | Number of the barbed needles | $L$ (mm) | $d$ (mm) | $\theta_1$ | $\theta_2$ | $h$ (mm) | $L_b$ (mm) | $t_1$ (mm) | The average insertion force range | The average SD's range |
|---|---|---|---|---|---|---|---|---|---|---|---|
| Barb front angle ($\theta_1$) | 1 | 7 | 180 | 3 | 90°, 100°,110°, 120°, 130°, 150°, 170° | 90° | 0.5 | 30 | 0.2 | $2.5 \leqslant IF \leqslant 4.5$ | $0.056 \leqslant SD \leqslant 0.19$ |
| Barb back angle ($\theta_2$) | 2 | 12 | 180 | 3 | 170° | 90°, 110°, 130°, 150°, 160°, 170° | 0.5 | 30 | 0.2 | $2.5 \leqslant IF \leqslant 4.5$ | $0.063 \leqslant SD \leqslant 0.17$ |
| Barb height ($h$) | 1 | 5 | 180 | 3 | 170° | 90° | 0.1, 0.2, 0.3, 0.4, 0.5 | 30 | 0.2 | $2.5 \leqslant IF \leqslant 4$ | $0.04 \leqslant SD \leqslant 0.11$ |
| Length of the barbed section ($L_b$) | 1 | 6 | 180 | 3 | 170° | 90° | 0.5 | 10, 20, 30, 40, 50, 60 | 0.2 | $2.5 \leqslant IF \leqslant 4.5$ | $0.07 \leqslant SD \leqslant 0.18$ |
| Thickness of the barb tip ($t_1$) | 1 | 5 | 180 | 3 | 170° | 90° | 0.5 | 40 | 0.05, 0.1, 0.15, 0.2, 0.25 | $4.5 \leqslant IF \leqslant 5$ | $0.11 \leqslant SD \leqslant 0.21$ |
| The scale study | 5 | 5 | 180, 150, 120, 90, 60 | 3, 2.5, 2, 1.5, 1 | 170° | 90° | 0.5, 0.42, 0.33, 0.25, 0.17 | 40, 33.3, 26.7, 20, 13.33 | 0.2, 0.17, 0.13, 0.1, 0.07 | $0.4 \leqslant IF \leqslant 4.5$ | $0.06 \leqslant SD \leqslant 0.14$ |
| Insertion tests into bovine liver tissue | 2 | 2 | 180, 120 | 3, 2 | 170° | 90° | 0.5, 0.33 | 40, 26.7 | 0.2, 0.13 | $1 \leqslant IF \leqslant 4.5$ | $0.15 \leqslant SD \leqslant 0.19$ |

defined, and their effects on insertion and extraction of the needle were studied. The parameter values were then modified experimentally based on the minimum insertion force in each set of experiments. First, the barb front angle influence on insertion force was investigated. The needle with the front angle ($\theta_1$) of 170° was found to have the minimum insertion force. Then, the back angle of the barb was modified based on both insertion and extraction forces. As shown in figures 10 and 11, the back angle ($\theta_2$) of 90° gave us the minimum insertion and extraction forces. Furthermore, the barb height ($h$) of 0.5 mm was observed to have the least insertion force among needles with different barb heights. Since the height of the barbs affects the bending stiffness of the needle, it is important to find a balance between the reduction in the insertion force and the stiffness. As shown in figure 12, the insertion force decreased by 17% using needle with barb height of 0.1 mm; this is interesting since the reduction in the needle stiffness is smaller (14%). The length of the barbed section impacts on the insertion force was investigated. It was found that the minimum insertion force was achieved using the needle with a barbed section length ($L_b$) of 40 mm (figure 13). The tip thickness of the barb ($t_1$) was the last design parameter which its effect on the insertion force results was studied. The results in figure 14 showed that there are relatively no changes in the insertion force for needles with different tip thicknesses. The insertion force decreased by 35% using needle with modified barb design values, which is more than what was achieved in our preliminary tests.

The size-scale effect on the insertion forces was explored using five different scales of the needle with modified barb values (figure 15). The results obtained for needles in different scales showed 21–26% decrease in the insertion force. It can be summarized that the reduction in the insertion force is due to the presence of the barbs, and not size of the needles.

To show the relevance for real applications, *ex vivo* insertion tests into bovine liver tissue were performed using needles with two different scales. The results of the insertions into liver tissue (figure 16) showed a 46% decrease in insertion force using barbed needles, which is even better than the results achieved from insertion tests into PVC gels.

Currently, insertion tests in some biological tissue, such as bovine liver and brain tissue, are being performed to further investigate the efficacy of the suggested design. Other future work includes manufacturing the true-scale bioinspired needles made of materials suitable for clinical applications. To manufacture a needle with barbs, we are following two different paths. The mesoscale manufacturing is the process of creating a product in the range of 0.1 mm to 5 mm, which is the range needed to carve the geometry of the barbs on the needle surface. This technique can be utilized to cut out the barbs on the surface of a conventional needle. The other path is to use a metal 3D printer to manufacture our needle. Both methods could be used for manufacturing hollow needles as well; however, the barb height for hollow needles should be smaller to maintain needle stiffness. The

stresses that build up during the printing, sintering, and infiltration processes, combined with the handling of parts in the green state, could result in warped or broken parts.

## Conclusions

Our results showed that it is feasible to achieve a 35% decrease in the insertion force by modifying the shape and geometries of the needles. In this study, bioinspired needles mimicking honeybee stingers were designed, modified, and tested.

The barb design parameters can be customized for different applications with different depths of insertion and/or mechanical properties of the tissue. The size-scale effect on insertion force results was studied. The results obtained from the scale study showed that having barbs decreases the insertion force (by 21–26%) regardless of the needle scale. Preliminary *ex vivo* insertion tests into bovine liver tissue were also performed to see the performance of the barbed needle in a biological tissue. The insertion force results for the insertion into bovine liver tissue represented a significant decrease in insertion force (as much as 46%) using barbed needles. The results acquired for both barbed and conventional needles during insertion into PVC gel and bovine liver tissue proved the effectiveness of the proposed needle design in decreasing the insertion force. Less invasive needles like the presented design can be utilized for insertion into fragile tissues like brain tissue.

## Acknowledgments

The authors also acknowledge Jonasan Younan Attia, David Gardell, and Kyle Jezler for their contributions. Finally, the authors would like to acknowledge Temple's Center of Excellence in Traumatic Brain Injury Research and the Department of Defense Congressionally Directed Medical Research Programs (CDMRP) program for the financial supports.

## ORCID iDs

Mohammad Sahlabadi https://orcid.org/0000-0002-1116-2895
Parsaoran Hutapea https://orcid.org/0000-0001-6917-1252

## References

[1] O'Leary M D, Simone C, Washio T, Yoshinaka K and Okamura A M 2003 Robotic needle insertion: effects of friction and needle geometry *2003 IEEE Int. Conf. on Robotics and Automation (Cat. No.03CH37422)* vol 2 pp 1774–80
[2] Yang S Y, O'Cearbhaill E D, Sisk G C, Park K M, Cho W K, Villiger M, Bouma B E, Pomahac B and Karp J M 2013 A bio-inspired swellable microneedle adhesive for mechanical interlocking with tissue *Nat. Commun.* **4** 1702
[3] Izumi H, Suzuki M, Aoyagi S and Kanzaki T 2011 Realistic imitation of mosquito's proboscis: electrochemically etched sharp and jagged needles and their cooperative inserting motion *Sens. Actuators,* A **165** 115–23
[4] Scali M, Kreeft D, Breedveld P and Dodou D 2017 Design and evaluation of a wasp-inspired steerable needle *Proc. SPIE* **10162** 2259978
[5] Burrows C, Liu F, Leibinger A, Secoli R and Baena F R 2017 Multi-target planar needle steering with a bio-inspired needle design *Advances in Italian Mechanism Science: Proc. of the First Int. Conf. of IFToMM Italy* ed G Boschetti and A Gasparetto (Cham: Springer) pp 51–60
[6] van Gerwen D J, Dankelman J and van den Dobbelsteen J J 2012 Needle-tissue interaction forces—a survey of experimental data *Med. Eng. Phys.* **34** 665–80
[7] Misra S, Reed K B, Douglas A S, Ramesh K T and Okamura A M 2008 Needle-tissue interaction forces for bevel-tip steerable needles *Proc. 2nd Biennial IEEE/RAS-EMBS Int. Conf. Biomedical Robotics and Biomechatronics* pp 224–31
[8] Henley D E, Leendertz J A, Russell G M, Wood S A, Taheri S, Woltersdorf W W and Lightman S L 2009 Development of an automated blood sampling system for use in humans *J. Med. Eng. Technol.* **333** 309–1902
[9] Brett P N, Parker T J, Harrison A J, Thomas T A and Carr A 1997 Simulation of resistance forces acting on surgical needles *Proc. Inst. Mech. Eng.* H **211** 335–47
[10] Brett P N, Harrison A J and Thomas T A 2000 Schemes for the identification of tissue types and boundaries at the tool point for surgical needles *IEEE Trans. Inf. Technol. Biomed.* **4** 30–6
[11] Healey A E, Evans J C, Murphy M G, Powell S, How T V, Groves D, Hatfield F, Diaz B M and Gould D 2005 *In vivo* force during arterial interventional radiology needle puncture procedures *Stud. Health Technol. Inform.* **111** 178–84
[12] Abolhassani N, Patel R and Moallem M 2006 Control of soft tissue deformation during robotic needle insertion *Minim. Invasive Ther. Allied Technol.* **15** 165–76
[13] Crouch J R, Schneider C M, Wainer J and Okamura A M 2005 Needle insertion with tissue relaxation Cs.Odu.Edu (https://doi.org/10.1.1.84.7867)
[14] Crouch J R, Schneider C M, Wainer J and Okamura A M 2005 A velocity-dependent model for needle insertion in soft tissue *Lect. Notes Comput. Sci.* **3750** 624–32
[15] Urrea F A, Casanova F, Orozco G A and García J J 2016 Evaluation of the friction coefficient, the radial stress, and the damage work during needle insertions into agarose gels *J. Mech. Behav. Biomed. Mater.* **56** 98–105
[16] DiMaio S P and Salcudean S E 2003 Needle insertion modeling and simulation *IEEE Trans. Robot. Autom.* **19** 864–75
[17] Naemura K, Uchino Y and Saito H 2007 Effect of the needle tip height on the puncture force in a simplified epidural anesthesia simulator *Proc. Annual Int. Conf. IEEE Engineering in Medicine and Biology* pp 3504–7
[18] Mahvash M and Dupont P E 2009 Fast needle insertion to minimize tissue deformation and damage *Proc. IEEE Int. Conf. Robotics and Automation* pp 3097–102
[19] Abolhassani N, Patel R V and Ayazi F 2007 Minimization of needle deflection in robot-assisted percutaneous therapy *Int. J. Med. Robot. Comput. Assist. Surg.* **3** 140–8
[20] Frick T B, Marucci D D, Cartmill J A, Martin C J and Walsh W R 2001 Resistance forces acting on suture needles *J. Biomech.* **34** 1335–40
[21] Meltsner M A, Ferrier N J and Thomadsen B R 2007 Observations on rotating needle insertions using a brachytherapy robot *Phys. Med. Biol.* **52** 6027–37
[22] Khalaji I, Hadavand M, Asadian A, Patel R V and Naish M D 2013 Analysis of needle-tissue friction during vibration-assisted needle insertion *IEEE Int. Conf. Intelligent Robots and Systems* pp 4099–104
[23] Clement R S, Unger E L, Ocón-grove O M, Cronin T L and Mulvihill M L 2016 Effects of axial vibration on needle insertion into the tail veins of rats and subsequent serial blood corticosterone levels *J. Am. Assoc. Lab. Anim. Sci.* **55** 204–12
[24] Tan L, Qin X, Zhang Q, Zhang H, Dong H, Guo T and Liu G 2017 Effect of vibration frequency on biopsy needle insertion force *Med. Eng. Phys.* **43** 71–6

[25] Okamura A M, Simone C and O'Leary M D 2004 Force modeling for needle insertion into soft tissue *IEEE Trans. Biomed. Eng.* **51** 1707–16
[26] Shergold O and Fleck N 2005 Experimental investigation into the deep penetration of soft solids by sharp and blunt punches, with application to the piercing of skin *J. Biomech. Eng.* **127** 838–48
[27] Stellman J T 2009 Development, production, and characterization of plastic hypodermic needles *Masters Thesis* Georgia Institute of Technology
[28] Mahvash M and Dupont P E 2010 Mechanics of dynamic needle insertion into a biological material *IEEE Trans. Biomed. Eng.* **57** 934–43
[29] Chebolu A, Mallimoggala A and Nagahanumaiah 2014 Modelling of cutting force and deflection of medical needles with different tip geometries *Proc. Mater. Sci.* **5** 2023–31
[30] Abolhassani N, Patel R and Moallem M 2007 Needle insertion into soft tissue: a survey *Med. Eng. Phys.* **29** 413–31
[31] Hirsch L, Gibney M, Berube J and Manocchio J 2012 Impact of a modified needle tip geometry on penetration force in subjects with diabetes *J. Diabetes Sci. Technol.* **6** 328–35
[32] Præstmark K A *et al* 2016 Pen needle design influences ease of insertion, pain, and skin trauma in subjects with type 2 diabetes *BMJ Open Diabetes Res. Care* **4** e000266
[33] Soper N J, Swanström L L and Eubanks S 2008 *Mastery of Endoscopic and Laparoscopic Surgery* (Baltimore, MD: Williams & Wilkins)
[34] Warren J D, Schott J M, Fox N C, Thom M, Revesz T, Holton J L, Scaravilli F, Thomas D G T, Plant G T, Rudge P and Rossor M N 2005 Brain biopsy in dementia *Brain* **128** 2016–25
[35] Hing J T, Brooks A D and Desai J P 2006 Reality-based needle insertion simulation for haptic feedback in prostate brachytherapy *Proc. IEEE Int. Conf. Robotics and Automation* vol 2006 pp 619–24
[36] Ling J, Song Z, Wang J, Chen K, Li J, Xu S, Ren L, Chen Z, Jin D and Jiang L 2017 Effect of honeybee stinger and its microstructured barbs on insertion and pull force *J. Mech. Behav. Biomed. Mater.* **68** 173–9
[37] Wu J, Yan S, Zhao J and Ye Y 2014 Barbs facilitate the helical penetration of honeybee (*Apis mellifera ligustica*) stingers *PLoS One* **9** e103823
[38] Hunt G J, Guzma E, Fondrk M K and Page R E 1998 Quantitative trait loci for honey bee stinging behavior and body size *Genet.* **148** 1203–13
[39] Casanova F, Carney P R and Sarntinoranont M 2014 *In vivo* evaluation of needle force and friction stress during insertion at varying insertion speed into the brain *J. Neurosci. Methods* **237** 79–89
[40] Li W, Belmont B and Shih A 2015 Design and manufacture of polyvinyl chloride (PVC) tissue mimicking material for needle insertion *Proc. Manuf.* **1** 866–78
[41] Xia H and Hirai T 2009 Space charge distribution and mechanical properties in plasticized PVC actuators *2009 IEEE Int. Conf. Mechatronics and Automation ICMA* pp 164–9
[42] Sahlabadi M, Gardell D, Younan Attia J, Khodaei S and Hutapea P 2017 Insertion mechanics of 3D printed honeybee-onspired needle prototypes for percutaneous procedure *ASME: Frontiers in Biomedical Devices, Design of Medical Devices Conf.* V001T08A020
[43] Sahlabadi M, Khodaei S, Jezler K and Hutapea P 2017 Insertion mechanics of bioinspired needles into soft tissues *Minim. Invasive Ther. Allied Technol.* (https://doi.org/10.1080/13645706.2017.1418753)
[44] Khodaei S, Sahlabadi M and Hutapea P 2017 Design of smart barb of honeybee-inspired surgery needle *ASME: Smart Materials, Adaptive Structures and Intelligent Systems. Development and Characterization of Multifunctional Materials; Mechanics and Behavior of Active Materials; Bioinspired Smart Materials and Systems; Energy Harvesting; Emerging Technologies* **1** V001T06A012
[45] Sahlabadi M, Khodaei S, Jezler K and Hutapea P 2017 Study of bioinspired surgery needle advancing in soft tissues *ASME: Smart Materials, Adaptive Structures and Intelligent Systems: Development and Characterization of Multifunctional Materials; Mechanics and Behavior of Active Materials; Bioinspired Smart Materials and Systems; Energy Harvesting; Emerging Technologies* **1** V001T06A016